J Solid State Electrochem (2010) 14:1101–1107
DOI 10.1007/s10008-009-0924-0

ORIGINAL PAPER

Synthesis and electrochemistry of multiwalled carbon nanotube films directly attached on silica substrate

Nikos G. Tsierkezos · Uwe Ritter

Received: 27 July 2009 / Revised: 11 August 2009 / Accepted: 11 August 2009 / Published online: 28 August 2009

Abstract Vertically aligned multiwalled carbon nanotubes (MWCNT) on silica substrate were selectively produced by the procedure of chemical vapor deposition (CVD). For the synthesis of the MWCNT films, either acetonitrile (ACN) or benzene (BZ) was used as carbon sources while ferrocene ($FeCp_2$) was adopted as catalyst. The packing organization of the aligned carbon nanotubes on the silica substrate, and thus the degree of disorder of the produced MWCNT films, was found to be different. Namely, the $MWCNT_2$ film, produced upon decay of BZ, seems to be more disordered compared to $MWCNT_1$, produced upon decomposition of ACN. In order to examine their prospective application as electrodes for the detection of electroactive compounds in organic solvent media, the techniques of cyclic voltammetry (CV) and electrochemical impedance spectroscopy (EIS) were employed. $FeCp_2$ was selected as the suitable standard electroactive substance for probing the fabricated MWCNT electrodes, in view of the fact that $FeCp_2$ undergoes a fast one-electron oxidation process forming the ferrocenium cation ($FeCp_2^+$), which is rather stable during the time scale of the experiments. All electrochemical experiments were performed in ACN as solvent medium including *n*-tetrabutylammonium hexafluorophosphate as supporting electrolyte at room temperature. The extracted CV and EIS results were compared with those obtained using glassy carbon electrode. The findings demonstrate the successful detection of $FeCp_2$ in ACN at both MWCNT films. However, among the films investigated, the electrode produced upon decay of BZ seems to be better capacitor, most probably due to its higher surface area as well as to its small film thickness. Evidently, the high degree of disorder, which has been observed for $MWCNT_2$, plays an important role for the increase of its effective surface area and thus, its capacitance. It is, however, very interesting that the more disorder $MWCNT_2$ film provides, the greater charge transfer resistance.

Keywords Chemical vapor deposition · Cyclic voltammetry · Electrochemical impedance spectroscopy · Heterogeneous electron transfer rate constant · Multiwalled carbon nanotubes

N. G. Tsierkezos (✉) · U. Ritter
Institut für Chemie, Elektrochemie und Galvanotechnik,
Fachgebiet Chemie, Technische Universität Ilmenau,
Weimarer Straße 25,
98693 Ilmenau, Germany
e-mail: nikos.tsierkezos@tu-ilmenau.de

Introduction

Besides being the basic element of life, carbon exhibits a richness of allotropes with diverse sorts of carbon–carbon bonds and different physical and chemical properties. The discovery of new forms of carbon, such as fullerenes and carbon nanotubes (CNT), offers many promising potential applications in the field of nanoscience and nanotechnology. The CNT, discovered in 1991 by Sumio Iijima [1], are allotropes of carbon with cylindrical nanostructure, which resemble graphite rolled up to a tube. Conceptually, single-walled carbon nanotubes (SWCNT) can be considered to be formed by the rolling of a single layer of graphite into a seamless cylinder. Consequently, a multiwalled carbon nanotube (MWCNT) can be similarly considered to be a coaxial assembly of cylinders of SWCNT, one within another. The method which was found to be efficient and selective for the synthesis of either SWCNT or MWCNT is the chemical vapor deposition (CVD) [2, 3]. The synthesis of CNT by means of CVD occurs through the decomposition of carbon-containing compounds on the surface of

nanometer-sized transition metal particles, such as iron, cobalt, or nickel, that act as catalyst for the decomposition of the carbon source and simultaneously serve for the CNT formation sites, upon which the CNT nucleate and grow. Organometallic compounds of iron, such as ferrocene ($FeCp_2$) or iron pentacarbonyl ($Fe(CO)_5$), were successfully used as catalysts for the CNT synthesis [4].

During the recent years, many researchers were involved in extensive theoretical and experimental investigation of CNT [5–9] since these materials, because of their unique cylindrical structure and their physical, chemical, mechanical, and electronic properties, are potentially useful in many applications in nanotechnology, electronics, optics, and other fields of materials science, as well as in architectural and biomedical field [10]. It is, therefore, not surprising that the CNT are excellent candidates for electron field emission sources, scanning probe tips, nanoelectronic devises, energy storage, actuators, as well as for chemical and biochemical sensors [11, 12].

The last years, CNT gained considerable attention in electrochemistry for the production of electrodes, since such electrodes have the ability to carry large current densities providing, therefore, fast electron transfer kinetics [13, 14]. Furthermore, the CNT electrodes have the advantage of reduced reaction potential and minimum surface fouling effects [15, 16]. The production of SWCNT electrodes is complicated and therefore, the development of such electrodes is somehow limited compared to that of MWCNT electrodes, which show promising electrochemical properties since they illustrate high electrical conductivity and excellent mechanical strength [17, 18]. A search in the literature revealed that many scientists carried out electrochemical studies on synthesized CNT films for the detection of either inorganic or organic compounds. In some cases, a functional group was also attached to one side of the nanotube film in order to facilitate the quick and specific response of the electrode [19]. Some representative articles are those of Xie et al. [20], Nguyen et al. [21], Ye et al. [22], Lamas-Ardisana et al. [23], and Snider et al. [24], in which synthesized MWCNT films were applied for the detection of the Pb^{2+}, NH_3, glucose, *p*-aminophenol, and insulin, respectively.

The aim of the present work is the fabrication of MWCNT films and the investigation of their electrochemical reactivity and sensitivity by means of CV and electrochemical impedance spectroscopy (EIS). For this purpose, two MWCNT electrodes with the same geometrical area (1.0 cm^2) were fabricated and tested. The $MWCNT_1$ and $MWCNT_2$ films tested in the present work were made up of silica substrate by the CVD procedure using $FeCp_2$ (1% *w*/*w*) as catalyst and ACN and BZ as carbon source materials. In order to evaluate the electrochemical performance of the constructed electrodes in organic solvent media, the standard redox system $FeCp_2^{+/0}$ was probed in ACN (0.20 mol L^{-1} *n*-tetrabutylammonium hexafluorophosphate ($TBAPF_6$)).

Experimental

Chemicals and solutions preparation

ACN (Merck, puriss grade) was distilled over Sicapent, redistilled over potassium carbonate, and stored over 0.4 nm molecular sieves. The specific conductivity of the purified ACN was found to be very small (5×10^{-8} S cm^{-1}). $FeCp_2$ (Fluka, purum grade) was recrystallized twice from heptane [25], while $TBAPF_6$ (Fluka, purum grade) was recrystallized twice from absolute ethanol and dried under reduced pressure at room temperature for 12 h [26]. The solids were stored under argon in Schlenk tubes. For the electrochemical experiments, a concentrated solution of $TBAPF_6$ (0.2 mol L^{-1}) in ACN was used for the preparation of the dilute solution of $FeCp_2$ (1×10^{-3} mol L^{-1}). All solutions were prepared under argon using Schlenk techniques.

Apparatus

The CVs were recorded using a computer-controlled system Zahner/IM6/6EX. The effect of the uncompensated resistance *iR* (where the symbol *i* represents the current and *R* the uncompensated resistance) was reduced by using the positive feedback technique. The measurements were carried out using a three-electrode cell configuration. The working electrodes used were either $MWCNT_1$, $MWCNT_2$ (geometrical area of silica substrate 1.0 cm^2), or glassy carbon (GC; effective surface area 0.24 cm^2); the counter electrode was Pt plate, while the reference electrode was Ag/AgCl (KCl saturated (sat.)). The real surface areas of the produced $MWCNT_1$ and $MWCNT_2$ films were determined as 0.71 and 0.92 cm^2, respectively. The measuring cell used was a three-compartment cell designed to minimize the distances between the electrodes having a total solution volume of ~20 mL. Before each measurement process, the solution was purged with high purity argon in order to eliminate interference from oxygen. The CVs were recorded in the potential region from −0.5 to +1.5 V vs Ag/AgCl (KCl sat.) with scan rates (*v*) ranging from 0.02 to 0.12 V s^{-1}. All measurements were carried out at the room temperature (294.15±0.5 K).

The EIS experiments were performed with a computer-controlled system Zahner/IM6/6EX. The EIS spectra were recorded at the reduction potential of $FeCp_2$ ($E_{1/2}$=0.42–0.45 V vs Ag/AgCl) by applying small AC amplitude (10 mV) in a wide frequency range (from 0.1 Hz to 50 kHz)

at the temperature of 294.15±0.5 K. All measurements were performed on either $MWCNT_1$, $MWCNT_2$, or GC working electrodes against the reference electrode Ag/AgCl (KCl sat.), with Pt plate as counter electrode. The EIS spectra were analyzed in order to determine the EIS parameters using the software Thales (version 4.15).

Scanning electron microscopy (SEM) pictures of the produced $MWCNT_1$ and $MWCNT_2$ films were obtained on a FEI/Philips (model XL30 ESEM) computer-controlled scanning electron microscope with an accelerating voltage of 10 kV and magnification factor of ×2000.

Preparation of the MWCNT films

Vertically aligned MWCNT (outer diameter ~4.0 nm) were selectively synthesized on silica (SiO_2) substrate in a furnace by catalytic CVD using $FeCp_2$ (1% *w*/*w*) as catalyst and either ACN or BZ as carbon sources. The $FeCp_2$ solution was introduced to the furnace through a syringe with a flow rate of 0.2 mL min^{-1} at the temperature of 900 °C. The synthesis process was performed using argon as carrier gas. The scheme of CVD apparatus and the catalyst method which was followed is reported in previous published articles [27, 28]. The synthesized MWCNT were characterized with SEM, thermogravimetric analysis, Raman spectroscopy, and transmission electron microscopy (TEM).

Results and discussion

Cyclic voltammetry

Representative CVs for the oxidation of $FeCp_2$ in ACN (0.2 mol L^{-1} $TBAPF_6$) on $MWCNT_1$, $MWCNT_2$, and GC working electrodes recorded in the potential range from −0.5 to +1.5 V vs Ag/AgCl at v=0.08 V s^{-1} are shown in Fig. 1. The electrochemical results for the investigated electrodes are presented analytically in Table 1. In all cases, the recorded CVs exhibit a pair of well-defined redox waves which are ascribed to the reaction $FeC\ p_2^+ + e^- \rightarrow FeC\ p_2$. Two characteristics reveal the different electrochemical behavior of the $FeCp_2^{+/0}$ couple on the investigated electrodes, the peak potential separation (ΔE), and the peak current (i_p).

For all electrodes investigated, the variation of the peak current with the square root of the scan rate was found to be linear (an example is given in inset of Fig. 2), and the ratio of the reductive current to the oxidative current (i_p^{red}/i_p^{ox}) was nearly unity. The peak current was found to be constant for several cycles indicating that there were no chemical reactions coupled with the electron transfer process. It is, however, obvious that the anodic and cathodic peak

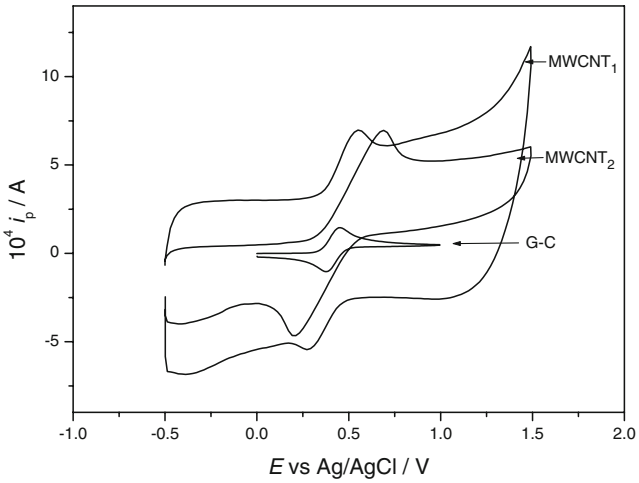

Fig. 1 CVs recorded for $FeCp_2$ (1×10^{-3} mol L^{-1}) in ACN (0.2 mol L^{-1} $TBAPF_6$) on $MWCNT_1$, $MWCNT_2$, and GC electrodes at v=0.08 V s^{-1}

currents are remarkably enhanced in the case of $MWCNT_1$ and $MWCNT_2$ electrodes compared to the peak currents observed on GC electrode. This observation can be ascribed to the increased active electrochemical surface area of the synthesized $MWCNT_1$ (0.71 cm^2) and $MWCNT_2$ (0.92 cm^2) electrodes. In the potential region, where no electron transfer between the solution and the working electrode occurs, the observed current is the responsible current for the formation at the interface (between solution and electrode surface) of the electric double layer. Thus, from the linear variation of the charging current with the potential scan rate, the double layer capacitance (C_{dl}) of the investigated MWCNT films can be determined. The determined C_{dl} values found to vary with the following order: $MWCNT_2$ (~0.8 μF)>$MWCNT_1$ (~0.2 μF)>GC (~0.1 μF). These values seem to agree with the C_{dl} values obtained from the EIS data (Table 1). As it is well known, the capacitance is directly proportional to the electrode active surface area and inversely proportional to the width of the charge separation layer. Consequently, the combined effect of a slim charge separation layer and a large surface electrode area leads to a high capacitance, which enables the double layer capacitor to receive, store, and release large supplies of electrical charge. The present results indicate that both synthesized MWCNT films comprise higher capacitances compared to that of the GC electrode. However, among $MWCNT_2$ and $MWCNT_1$ electrodes, the first electrode seems to be a greater capacitor, due to its higher effective surface area (0.92 cm^2) and its smaller electrode thickness (~19 μm; Fig. 3b). This ability of the $MWCNT_2$ film is probably connected to the restricted "packing organization" of the aligned carbon nanotubes, and thus to the higher degree of "disorder" which can be observed in this electrode. To be precise, it has been

Table 1 Anodic (E_p^{ox}) and cathodic (E_p^{red}) peak potentials, peak potential separations (ΔE_p), anodic peak current (i_p^{ox}), cathodic and anodic peak current ratios (i_p^{red}/i_p^{ox}), half-wave potentials ($E_{1/2}$), transfer coefficients (a), heterogeneous electron transfer rate constants (k_s), charge transfer resistance (R_{ct}), and double layer capacitance (C_{dl}) for the oxidation of $FeCp_2$ (1×10^{-3} mol L^{-1}) in ACN (0.2 mol L^{-1} $TBAPF_6$) on $MWCNT_1$, $MWCNT_2$, and GC electrodes at the scan rate of v=0.08 V s^{-1}

Electrode	$MWCNT_1$[d,e,f]	$MWCNT_2$[d,e,g]	GC
E_p^{ox}/V[a]	0.575	0.710	0.455
E_p^{red}/V[a]	0.299	0.192	0.376
ΔE_p/V	0.276	0.518	0.079
10^4 i_p^{ox}/A	3.7	6.3	1.4
i_p^{red}/i_p^{ox}	0.95	0.95	0.99
$E_{1/2}$/V[a]	0.437	0.451	0.416
a	0.50	0.50	0.50
10^3 k_s/cm s^{-1}[b,c]	0.65 (1.10)	0.12 (0.20)	18.6 (23.5)
R_{ct}/Ω	162	562	12.0
10^9 C_{dl}/F	167	910	154

[a] All potentials are reported vs Ag/AgCl (KCl sat.) reference electrode

[b] The k_s values were determined from the relation given by Nicholson [33]: $\psi = (D_o/D_R)^{a/2}k_s(n\pi FvD_o/RT)^{-1/2}$, where ψ is kinetic parameter, a the charge transfer coefficient, D_o and D_R the diffusion coefficients of the oxidized and reduced species, respectively ($D_o \approx D_R$, $D_o=2.24\times10^{-5}$ cm^2 s^{-1}) [39], and n the number of the electrons involved in the reaction (n=1)

[c] The k_s values given in parenthesis were determined according to the ψ parameters reported by Brett and Brett [40]

[d] The geometrical area of the fabricated MWCNT electrodes was 1.0 cm^2

[e] The active surface areas of the $MWCNT_1$ and $MWCNT_2$ films were 0.71 and 0.92 cm^2, respectively

[f] The $MWCNT_1$ electrode was produced by using ACN as carbon source

[g] The $MWCNT_2$ electrode was produced by using BZ as carbon source

observed from the SEM images that in changing the carbon source material, the arrangement of the formed MWCNT was modified. As it can be seen from the SEM images given in Fig. 3, when ACN is used as carbon precursor, the "packing organization" of the aligned MWCNT on the film is quite enhanced (Fig. 3a), while the MWCNT arrangement becomes rather worse when BZ is used as carbon source material (Fig. 3b). It can be, therefore, concluded that the high degree of "disorder" of $MWCNT_2$ plays an important role for the increase of its effective surface area and thus its capacitance.

The anodic (E_p^{ox}) and cathodic (E_p^{red}) peak potentials of the $FeCp_2^{+/0}$ couple on $MWCNT_1$ and $MWCNT_2$ electrodes differ and vary with the scan rate, and consequently, the half-wave potentials ($E_{1/2}$), taken as the average value of E_p^{ox} and E_p^{red} [29], show some discrepancies. For example, the determined $E_{1/2}$ values at v=0.08 V s^{-1} for $MWCNT_1$

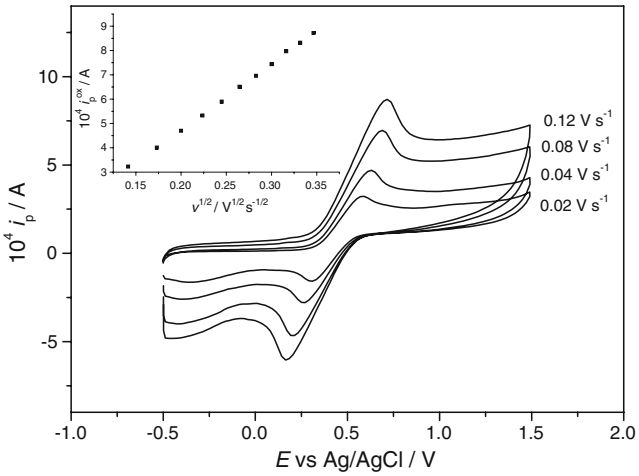

Fig. 2 CVs recorded on $MWCNT_2$ electrode showing the effect of the scan rate on the electrochemistry of $FeCp_2$ (1×10^{-3} mol L^{-1}) in ACN (0.2 mol L^{-1} $TBAPF_6$). *Inset*: the variation of the oxidative peak current (i_p^{ox}) with the square root of scan rate ($v^{1/2}$) observed on $MWCNT_2$ electrode in the scan rate range from 0.02 to 0.12 V s^{-1}

and $MWCNT_2$ electrodes lie at 0.437 V and 0.451 V vs Ag/AgCl, respectively, while the $E_{1/2}$ value obtained for GC electrode is shifted toward less positive potentials ($E_{1/2}$=0.416 V vs Ag/AgCl; Table 1). Anyhow, the transfer coefficient (a), determined from the relation: $a = \left(E_p^{ox} - E_{1/2}\right)/\left(E_p^{ox} - E_p^{red}\right)$ [30], was found to be equal to 0.5 in all cases. Not surprising, the investigated MWCNT electrodes exhibit variable and quite large peak potential separations (ΔE>0.270 V) compared to the peak separation observed for GC electrode (ΔE=0.079 V), which seems to be very close to the expected theoretical value for a reversible one electron transfer and diffusion-controlled process (ΔE=0.060 V at 298.15 K). Since the peak separation gives an estimation of the kinetic of the electron transfer process and thus it can be used for the determination of the heterogeneous electron transfer rate constant (k_s), one can initially consider that the smaller the peak separation, the higher the electron transfer constant rate. It is, though, possible that such large peak separation values can also be attributed to uncompensated resistance effects, which in this case seem to be rather significant. Since the "slow" electron transfer kinetic does not depend on the analyte concentration, in contrast to the uncompensated resistance which is concentration-dependent, the two effects were differentiated by running the experiments at different concentrations. The results reveal that by increasing the $FeCp_2$ concentration even higher, ΔE values are obtained, indicating, therefore, that the large ΔE values observed for MWCNT films can be attributed to resistance that still remains uncompensated. In this point, it must be mentioned that during the experiments, only the 85% of the uncompensated resistance was compensated in order to avoid overcompensation and consequently, circuit oscillation.

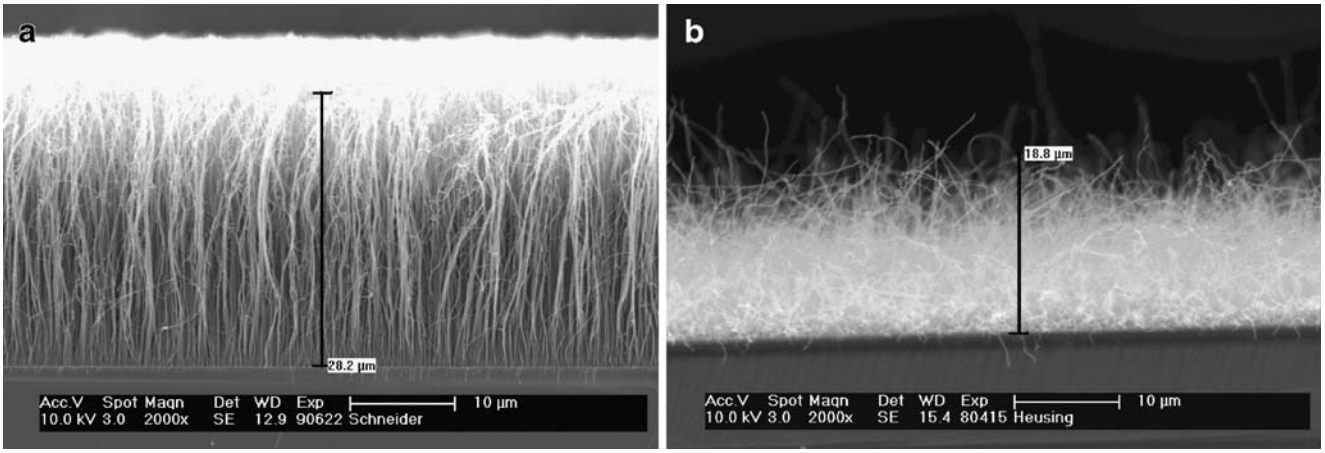

Fig. 3 Typical SEM images of MWCNT electrodes synthesized by means of CVD upon decomposition of ACN (**a**) and BZ (**b**), using $FeCp_2$ as catalyst (1% *w*/*w*; the SEM pictures were obtained with an accelerating voltage of 10 kV and magnification factor of ×2000). The average thickness of the synthesized MWCNT film was ~28 μm (ACN) and ~19 μm (BZ)

Obviously, the k_s values determined by using the obtained ΔE values can provide only an approximate value of the rate of the electron transfer process occurring on MWCNT films. Anyhow, considering that the amount of the resistance which was not compensated is approximately the same for both MWCNT films (since the same conditions were applied for the experiments), the difference in ΔE values observed for these two films reflects their dissimilar rates for the electron transfer process. Accordingly, for informative reasons, the k_s values were determined by following the treatment described by Nicholson [31] (Table 1). The k_s values suggest that the electron transfer process on GC electrode is extremely faster $k_s \approx 19\times10^{-3}$ cm s^{-1} compared to the electron transfer procedure occurs on either $MWCNT_1$ $k_s \approx 0.7\times10^{-3}$ cm s^{-1} or $MWCNT_2$ $k_s \approx 0.1\times10^{-3}$ cm s^{-1} electrodes, which is obviously fairly slow. It is, however, very interesting to mention in this point that the greatest ΔE value, and thus the smallest k_s value, was observed for $MWCNT_2$, which was produced by using BZ as carbon source. $MWCNT_1$, which was produced upon decomposition of ACN, reveals obviously smaller ΔE and consequently larger k_s value. These results can be connected to the different arrangement and consequently the different degree of "disorder" of the aligned MWCNT which was observed in these electrodes. It is therefore probable that the "packing organization" of the aligned MWCNT affects the electrochemical behavior of the constructed electrodes, since it plays a main role for the interactions between the electroactive compound and the electrode.

The above CV results signify a reversible behavior of $FeCp_2^{+/0}$ couple on GC electrode while the process tends to be quasireversible on either $MWCNT_1$ or $MWCNT_2$. The single oxidation and reduction peaks for $FeCp_2$ which have been observed in the present work indicate that only one type of $FeCp_2$ exists in the investigated systems, namely the bulk or "free" $FeCp_2$. In contrast to the results found in the present work, in the study of Zheng et al. [32] which has been performed in aqueous solutions, double CV peaks of $FeCp_2$ were observed on MWCNT films, which were assigned to be attributed to the bulk or "free" and adsorbed $FeCp_2$. According to that report, $FeCp_2$ has a strong adsorption capability on MWCNT electrodes, while its ability to be adsorbed on GC is rather insignificant or negligible. That behavior was assigned to be attributed to the π–π interactions between $FeCp_2$ and MWCNT [33]. Obviously, the present work confirms that $FeCp_2$ exhibits different behavior in organic solvent media, such as ACN, than in aqueous solutions.

Electrochemical impedance spectroscopy

EIS is an effective method to probe the interfacial properties such as electron transfer resistance and double-layer capacitance of the electrodes, and therefore, it was considered useful to be used in order to complement the characterization of the surfaces of the fabricated MWCNT electrodes [34]. The EIS spectra (Nyquist plots) recorded on $MWCNT_1$, $MWCNT_2$, and GC electrodes are presented in Fig. 4. As it can be observed in Fig. 4, there are some significant differences in the recorded EIS spectra. Analytically, it can be observed that the Nyquist plot obtained for GC electrode reveals a liner impedance locus, namely a Warbung impedance response, with an angle of about 45° to the z_{re}-axis. The early increase of the imaginary part of impedance and the absence of any indication of a semicircle at high frequencies indicate that the interfacial charge transfer process is very fast on the GC

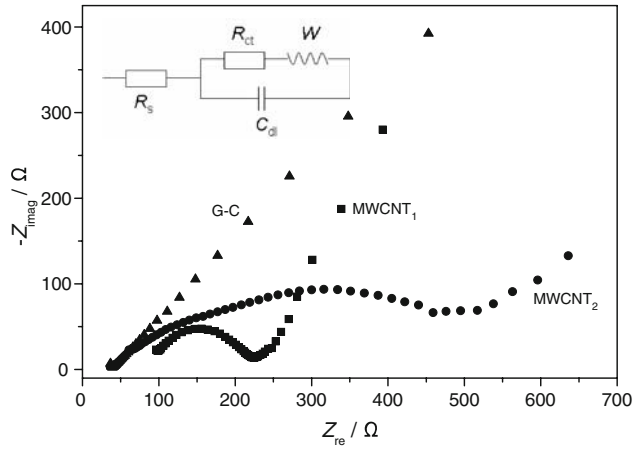

Fig. 4 EIS spectra recorded for $FeCp_2$ (1×10^{-3} mol L^{-1}) in ACN (0.2 mol L^{-1} $TBAPF_6$) on $MWCNT_1$, $MWCNT_2$, and GC electrodes in the frequency range from 0.1 Hz to 50 kHz at the formal potential of the $FeCp_2^{+/0}$ redox couple. *Inset*: the equivalent circuit used for fitting the EIS data. The symbols are denoted as follows: R_s electrolyte resistance, C_{dl} double layer capacitance, R_{ct} charge transfer resistance, and W Warbung impedance

electrode [35]. Such response is indicative of a reversible diffusion-controlled electron transfer process [36]. This behavior confirms that the heterogeneous charge transfer rate constant (k_s) of the $FeCp_2^{+/0}$ redox couple on GC electrode must be greater than 0.01 cm s^{-1}. However, the Nyquist plots obtained for the investigated $MWCNT_1$ and $MWCNT_2$ electrodes show the appearance of a very well defined semicircle terminating to a line. In details, the EIS spectra include a semicircle portion, observed at higher frequencies, that corresponds to the electron transfer limited process, followed by a linear part, characteristic of the lower frequency, attributable to a diffusionally limited electron transfer [37]. The respective semicircle diameter, which can be obtained by extrapolation of the semicircles on the z_{re}-axis, corresponds to the charge transfer resistance (R_{ct}) at the electrode surface. Such parameter provides an estimation not only of the response of the electron transfer but also of the sensitivity of the electrode. According to the theory, the development of such semicircles exhibit a barrier for the interfacial electron transfer and it can be attributed to an increase of the passivity of the surface of the electrode through a film formation, namely the formation of a coating. The presence of a coating at the electrode surface is expected to slow down the interfacial charge transfer kinetics, which is reflected by an increase of the electron transfer resistance. Anyhow, the appearance of semicircle can be also attributed to partial degradation of the MWCNT film on the surface of the SiO_2 substrate [38].

The experimental impedance data were fitted according to the Randles electrical circuit model. The Randles circuit, shown in the inset of Fig. 4, is used very often in order to describe electron transfer reactions at a planar electrode/film surface and includes a resistance in series with a parallel combination of a capacitive path and charge transfer path. The series resistance (R_s) represents the resistance of the electrolyte fluid plus the resistance of cables and wires connecting the electrode to the instrument, the double-layer capacitance (C_{dl}) is made up of charges in working electrode and ions in the solution, the charge-transfer resistance (R_{ct}) represents current flow via redox reactions at the electrode–fluid interface (is kinetically controlled), and W is a Warburg impedance element which arises physically from mass transport limits of ions in the solution (is mass-transfer controlled). The chosen equivalent circuit was found to fit the experimental impedance values. As can be seen in Fig. 5, in which a representative Bode plot obtained for the $MWCNT_1$ electrode is presented, the experimental and the simulated values seem to agree, confirming, therefore, that the Randles equivalent circuit represents the investigated systems. Anyhow, the obtained error from the simulation of the experimental EIS data by using the Randles circuit was found to be about 0.2% in all cases, and therefore, it can be considered acceptable. The determined EIS parameters are included in Table 1. The C_{dl} values decrease with the following order: $MWCNT_2$ (0.910 μF)>$MWCNT_1$ (0.167 μF)>GC (0.154 μF). The C_{dl} values slightly differ from the corresponding C_{dl} values determined from the CVs (see below). The extracted results suggest $MWCNT_2$ as the greater capacitor, probably because of its higher effective surface area (0.92 cm^2) and its smaller electrode thickness (19 μm) which both result from the high degree of "disorder" of the aligned carbon nanotubes on the surface of this film. The R_{ct} values were found to decrease with the following order: $MWCNT_2$ (R_{ct}=562 Ω)>$MWCNT_1$ (R_{ct}=162 Ω)>GC (R_{ct}=12 Ω). The results indicate that the

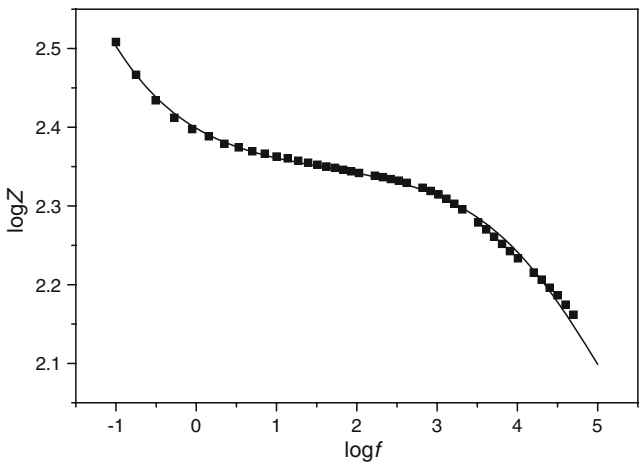

Fig. 5 Bode plot for $MWCNT_1$. The *peaks* represent the experimental impedance values, while the *solid line* represents the simulated values (software Thales, version 4.15)

tendency for the electron transfer is amplified on going from $MWCNT_2$ to GC electrode. In this point, it must be mentioned that similar trend was observed through the determined k_s values from the CV data (see above). It can be, therefore, concluded that the high degree of "disorder" on the surface of $MWCNT_2$ film leads to weakening of the interactions between the electroactive compound and the electrode and consequently, results to interruption of the electron transfer.

Conclusions

The aim of the present research was to study the electrochemical properties of MWCNT films created on silica substrate by means of CVD, using either ACN or BZ as carbon sources and $FeCp_2$ as catalyst. The electrochemical properties of the produced MWCNT films were investigated with the methods of CV and EIS by probing the $FeCp_2^{+/0}$ couple in ACN. $FeCp_2$ was successfully detected at the synthesized MWCNT films. The half-wave potential of the $FeCp_2^{+/0}$ couple shifts positively, and the peak current remarkably increases on the synthesized MWCNT electrodes compared to the GC electrode. SEM images revealed that the degree of the "packing organization" of the aligned carbon nanotubes on the film created upon decay of ACN is much greater compared to that produced upon decomposition of BZ. The last incident affects the extent of the interactions between $FeCp_2$ and electrodes and consequently, influences the electrochemical properties of the created films. The results indicated that the high-ordered $MWCNT_1$ reveals smaller charge transfer resistance and behaves as weaker capacitor compared to the less-ordered $MWCNT_2$, which causes higher R_{ct} and works as better capacitor.

Acknowledgments The authors would like to thank Mrs. D. Schneider and Mrs. S. Heusing (TU Ilmenau).

References

1. Iijima S (1991) Nature 354:56
2. Cassell AM, Raymakers JA, Kong J, Dai H (1999) J Phys Chem B 103:6484
3. Li YL, Kinloch IA, Windle AH (2004) Science 304:276
4. Bladh K, Falk LKL, Rohmund F (2000) Appl Phys A 70:317
5. Heyden A, Düren T, Keil FJ (2002) Chem Eng Sc 57:2439
6. Corrias M, Caussat B, Ayral A, Durand J, Kihn Y, Kalck Ph, Serp Ph (2003) Chem Eng Sc 58:4475
7. Kuwana K, Li T, Saito K (2006) Chem Eng Sc 61:6718
8. Moisala A, Nasibulin AG, Brown DP, Jiang H, Khriachtchev L, Kauppinen EI (2006) Chem Eng Sc 61:4393
9. Alexiadis A, Kassinos S (2008) Chem Eng Sc 63:2047
10. Oh ES (2004) Korean J Chem Eng 21:494
11. Jung DH, Kim BH, Ko YK, Jung MS, Jung S, Lee SY, Jung HT (2004) Langmuir 20:8886
12. Liu XL, Han S, Zhou CW (2006) Nano Lett 6:34
13. Campbell JK, Sun L, Crooks RM (1999) J Am Chem Soc 121:3779
14. Cai H, Cao X, Jiang Y, He P, Fang Y (2003) Anal Bioanal Chem 375:287
15. Sherigara BS, Kutner W, Souza FD (2003) Electroanal 15:753
16. Pan D, Chen J, Yao S, Tao W, Nie L (2005) Anal Sci 21:367
17. Punbusayakul N, Talapatra S, Ci L, Surareungchai W, Ajayan PM (2007) Electrochem Solid-State Lett 10:13
18. Kim YA, Muramatsu H, Hayashi T, Endo M, Terrones M, Dresselhaus MS (2004) Chem Phys Lett 398:87
19. Huang X, Sun Y, Wang L, Meng F, Liu J (2004) Nanotechnology 15:1284
20. Xie X, Gan T, Sun D, Wu K (2008) Fullerenes. Nanotubes Carbon Nanostruct 16:103
21. Nguyen LH, Phi TV, Phan PQ, Vu HN, Nguyen-Duc C, Fossard F (2007) Physica E 37:54
22. Ye JS, Wen Y, De Zhang W, Ming Gan L, Xu GQ, Sheu FS (2004) Electrochem Commun 6:66
23. Lamas-Ardisana PJ, Queipo P, Fanjul-Bolado P, Costa-Garcia A (2008) Anal Chim Acta 615:30
24. Snider RM, Ciobanu M, Rue AE, Cliffel DE (2008) Anal Chim Acta 609:44
25. Quirk PF, Kratochvil B (1970) Anal Chem 42:535
26. Hartl F, Mahabiersing T, Le Floch P, Mathey F, Ricard L, Rosa P, Záli S (2003) Inorg Chem 42:4442
27. Rao CNR, Sen R, Satishkumar BC, Govindaraj A (1998) Chem Commun 1525
28. Satishkumar BC, Govindaraj A, Rao CNR (1999) Chem Phys Lett 307:158
29. Carter MT, Rodriguez M, Bard AJ (1989) J Am Chem Soc 111:8901
30. Aoki K, Kaneko H, Nozaki K (1988) J Electroanal Chem 247:29
31. Nicholson RS (1965) Anal Chem 37:1351
32. Zheng D, Li H, Lu B, Xu Z, Chen H (2008) Thin Solid Films 516:2151
33. Li YF, Hatakeyama R, Kaneko T, Izumida T, Okada T, Kato T (2006) Nanotechnology 17:4143
34. Gabrielli C (1990) Use and application of electrochemical impedance techniques. Solartron, Farnborough
35. Rodriguez Nieto JF, Tucceri RI, Posadas D (1996) J Electroanal Chem 403:241
36. Mohran HS (2005) Am J Appl Sci 2:1629
37. Bardea A, Patolsky F, Dagan A, Willner I (1999) Chem Commun 21
38. Barbero C, Tucceri RI, Posadas D, Silber JJ, Sereno L (1995) Electrochim Acta 40:1037
39. Tsierkezos NG (2007) J Solution Chem 36:289
40. Brett CMA, Brett AMO (1988) Electroanalysis. Oxford University Press Inc, New York